Green synthesis, characterization and evaluation of the degradation potential of bimetallic copper-zinc nanoparticles for azo dye using Red Sage (*Lantana camara*)

Bhatti Laxmi, Panchal Kamaljit, Bhatia Divya, Kumar Rajesh and Khatak Sunita*
Department of Biotechnology, University Institute of Engineering and Technology, Kurukshetra University, Kurukshetra-136119, Haryana, INDIA
*sunitakhatak2019@gmail.com

Abstract
Nanoparticles have expanded their horizon in different sectors like cosmetics, medicines and agrochemicals. The synthesis of nanoparticles using plant extract is a very efficient, cost-effective, useful and ecologically friendly technology. Lantana camara is one of the potential plants for biosynthesis of nanoparticles due to its easy availability. In the present study, the Lantana camara plant extract was exploited for synthesis of copper, zinc and copper-zinc nanoparticles. UV-Vis spectroscopy, Fourier Transform Infrared and Dynamic light scattering were performed for characterization of synthesized nanoparticles. UV-Vis spectroscopy provided corroborating evidence, affirming the optical properties of the zinc, copper and copper-zinc nanoparticles with an observed absorption peak at 398, 570 and 437 nm. X-ray diffraction analysis unequivocally confirmed the crystalline nature of the zinc, copper and copper-zinc nanoparticles, revealing an average particle size of 18.7, 37.0 and 14.4 nm.

Further insights from Field emission scanning electron microscopy elucidated that the nanoparticles exhibited an irregular shaped with agglomeration, displaying particle sizes ranging around 38.8 nm. The polydispersity index of synthesized copper, zinc and copper-zinc nanoparticles was 0.486, 0.344 and 0.243 with net surface charge of -35.56, -34.87 and 34.13mV which infers to the stability of nanoparticles. Biosynthesized copper, zinc and copper-zinc nanoparticles revealed potent dye degradation potential against Congo red dye.

Keywords: X-ray diffraction, Polydispersity Index, Degradation.

Introduction

Medicinal plants have been utilized to combat illness since the dawn of civilization. Most current medications are generated from plant sources or their derivatives for various medicaments and they are widely used in the pharmaceutical business[42]. It is reported that about 50% of all fatality in developing countries is mainly due to the current infectious diseases[22]. This circumstance has led researchers to create effective new antibacterial drugs. Exploration of medicinal plants for curative purposes is primarily based on existing traditional knowledge from specialists and the local population[31,35].

Due to its exceptional healing potential, *Lantana camara* of *Verbenaceae* family is a medicinal aromatic plant and occurs in most parts of the world as an evergreen notorious weed species. It is also regarded as an ornamental garden plant. It is commonly utilized in traditional medicinal practices to address a variety of health conditions. Almost all plant parts are used to treat a variety of human illnesses including measles, chicken pox, tetanus, malaria, malignancies, asthma, ulcers, fevers, eczema, skin rashes, heart problems and rheumatism[13,20]. In addition, *L. camara* leaf extracts and essential oil have larvicidal, antioxidant, anti-inflammatory, analgesic, antidiabetic, hypolipidemic, anthelmintic, wound healing and antipyretic characteristics[34,42].

The plant's therapeutic potential is attributed to the presence of numerous bioactive phytocompounds such as terpenoids, alkaloids, flavonoids, polyphenols, glycosides and steroids as significant phytoconstituents[17]. The plant's therapeutic potential is because of numerous bioactive phytocompounds such as terpenoids, alkaloids, flavonoids, polyphenols, glycosides and steroids as significant phytoconstituents[17]. Certainly, additional research is needed to investigate the potential benefits of *Lantana camara* in addressing a variety of health conditions.

Nanotechnology is the utilization of nanoscale materials with diameters ranging from 1 to 100 nm.[10] Operating with nanomaterial has allowed researchers to have a much better understanding of biology. The green synthesis of nanoparticles has significantly reduced the use of physical and chemical processes.

Researchers are increasingly using the green synthesis approach because it uses less harmful chemicals, is environmentally benign and allows for the production of nanoparticles in a single step. As a result, it is important to note that nanoparticle production using plants has significant advantages over other biological systems because plants are readily available and the biogenic synthesis procedure is less costly and time-consuming than biosynthesis using fungal sources, which requires very long, tedious and aseptic culture. Nanoparticles have been synthesized using biological organisms like bacteria, yeast, fungus along with plant extracts obtained from plant parts. The active

biological ingredient found in plant parts such as enzyme acts as a reducing and capping agent, lowering the overall cost of the synthesis process[40].

Lantana camara has been utilized for synthesis of various nanoparticles which include silver, gold, copper, zinc, iron etc. copper and zinc nanoparticles have been shown to have various environmental remediation potential. This present work reports the synthesis of zinc, copper and copper-zinc based nanoparticles prepared from an important medicinal plant, *Lantana camara*. Characterization of Zn, Cu and Cu-Zn NPs was done by using UV–Visible spectroscopy, XRD, SEM, EDX and DLS. Dye degradation activity of synthesized zinc, copper and copper-zinc was also evaluated.

Material and Methods

Preparation of the Plant leaf extract: The harvested *Lantana camara* leaves underwent a thorough washing with de-ionized water, until no foreign material remained and then oven dried at 50ºC till moisture needs to be completely removed by evaporation and ground to fine powder[19,39]. 10g of leaf was ground to fine powder and stirred with 100 ml of deionized water at 85ºC for 20 min[31,38]. The leaf extract was filtered with Whatmann no.1 filter paper and the filtrate was stored at 4ºC. This extract fulfilled a dual purpose both as a reducing and as stabilizing agent.

Synthesis of Zn Nanoparticles: An aqueous solution of 90ml (0.025M) zinc nitrate hexahydrate was added to 10ml of *Lantana camara* leaf extract and the mixture was stirred with a magnetic stirrer at room temperature. The color of the solution changed from colourless to cream colour solution. The primary method of identifying the creation of zinc nanoparticles was color change[26]. The nanoparticles were extracted by heating the solution at 75°C and till it converted to powdered zinc oxide nanoparticle. After that, the mixture is reduced to a paste with a bright yellow color by boiling it[33].

Synthesis of Cu Nanoparticles: For Cu NPs synthesis, 10ml of plant extract using leaves was mixed with 90 mL of 0.025M copper sulphate pentahydrate solution with constant stirring at 75°C. Colour change of the solution was monitored from bluish to light green[9]. The solid portion in the product was separated by centrifugation at 3000 rpm for 20 min at 4°C, washed four times with deionized water and ethanol, the pellet was dried in a hot air oven.

Synthesis of Cu-Zn bimetallic NPs: To synthesize bimetallic nanoparticles (Cu-Zn), a solution was prepared by transferring 0.025M zinc nitrate hexahydrate and 0.025M copper sulphate into 90ml of deionized water. Following that, 10ml of extract was gradually added to the mixture. The resulting solution underwent continuous stirring on a magnetic stirrer at 75°C for duration of 3h, during which the solution was observed for colour transition from light blue to dark green. After this process, the solution was subjected to centrifugation at 3000 rpm using for 20 min at 4°C, after that NPs were washed four times with distilled water and ethanol to remove water impurities and then nanoparticles were stored in dry bottles for further analysis. The collected mixture was then dried and calcined at 400°C to form bimetallic nanoparticles[39].

Optimization study for bimetallic Cu-Zn nanoparticles: The effect of various contents on the synthesis of Cu-Zn NPs was investigated using different concentrations of copper sulphate and zinc nitrate (10mM, 15mM, 20mM, 25mM, 30mM). The surface plasmon resonance (SPR) peaks were obtained using a spectrophotometer. The effect of different concentrations (1:9, 2:8, 3:7, 4:6, 5:5) of *Lantana camara* leaves extract to Cu-Zn salt on nanoparticle synthesis was determined by SPR and UV-Vis analysis. The effect of pH (2, 4, 6, 8, 10), temperatures (35°C, 45°C, 55°C, 65°C, 75°C) and incubation times (30 minutes, 1h, 2h, 3h, 12h) on nanoparticle synthesis was measured spectrophotometrically. To determine the stability of the synthesized Cu-Zn NPs, they were stored at room temperature.

Characterization of nanoparticles: The surface plasmon resonance of synthesized Cu-Zn NPs was investigated using UV spectroscopy at a 300-600 nm wavelength. The analysis of the derived material's structure and elemental composition was conducted through Field emission scanning electron microscope (FESEM) and EDAX. The hydrophobic particle size, Zeta potential and polydispersity index were predicted using DLS. The use of an XRD enabled the investigation of crystallinity and phase purity[25]. X-ray diffraction (XRD) analysis of nanoparticles was carried out to study the crystalline structure in a powder XRD system equipped with CuKα radiation. The average size based on XRD was measured using the Debye–Scherrer equation i.e. $D=K\lambda / \beta Cos\theta$. Then it was subjected to FT-IR spectrometer analysis to capture the spectrum spanning from 500 to 4000 cm^{-1} to examine the functional groups present.

Dye Degradation Activity: The photo catalytic dye degradation potential of Cu, Zn and Cu-Zn NPs was evaluated for Congo red. To prepare the stock solution, add 0.1% dye to 100ml of distilled water. To make a total volume of 3 ml, combine 20µl of dye and 50µl of different NP concentrations with distilled water. Then, the solution was kept in sunlight. After this, a UV-Vis spectrophotometer was used to measure the change in intensity of color at 498 nm. The % degradation of dyes was estimated as follows:

Dye degradation % - Ao -At /Ao ×100

where At means absorbance at t and Ao denotes absorbance at zero time.

Results and Discussion

Visible Color Change of the Solution: Zinc, copper and bimetallic copper-zinc nanoparticles were successfully

synthesized using an herbal plant leaf extract derived from *Lantana camara*. Review of literature revealed that plant extracts not only facilitate controlled synthesis but also play roles as stabilizing and capping agents[4]. This convergence of results emphasizes the viability and potential of using plant extracts for eco-friendly nanoparticles synthesis[14]. Zinc, copper and copper-zinc nanoparticles formation was initially confirmed by change in color of solution. Color changes in solutions are caused by chemical compounds such as alkaloids, saponins, flavonoids and steroids in plant extracts[32], which act as reducing agent, converting copper-zinc ions to copper-zinc atoms.

Visually plant extract was treated with (0.025M) Cu, Zn and copper-zinc aqueous solution showing a color change from blue to light bluish green, colourless to light yellow, bluish solution to dark green colored solution respectively as shown in figure 1(b, c, d). Copper-zinc nanoparticles' greenish color results from surface plasmon resonance in aqueous solution. Ramesh et al[36] and Singh et al[39] also reported similar changes in the color during nanoparticles formation.

Optimization of different parameters: For efficient synthesis of Cu-Zn nanoparticles, effect of incubation time, effect of pH, effect of temperature, effect of ratio of plant extracts to Cu-Zn solution, effect of concentration of Cu-Zn solution on Cu-Zn nanoparticles formation was investigated and the optimum conditions for the reaction were selected as shown in figure 2. UV-Visible spectrums analysis was used to monitor the effect of incubation time on Cu-Zn nanoparticles concentration in the reaction mixture at different incubation time with a change in color of the solution[44]. The absorbance peak intensity increases gradually, then become constant. After a particular time of 3 hour, no significant change was observed in synthesis of Cu-Zn nanoparticles.

a) b) c) d)

Figure 1: a) *Lantana camara* plant b) Cu solution c) Zn solution d) Cu-Zn nanoparticle solution

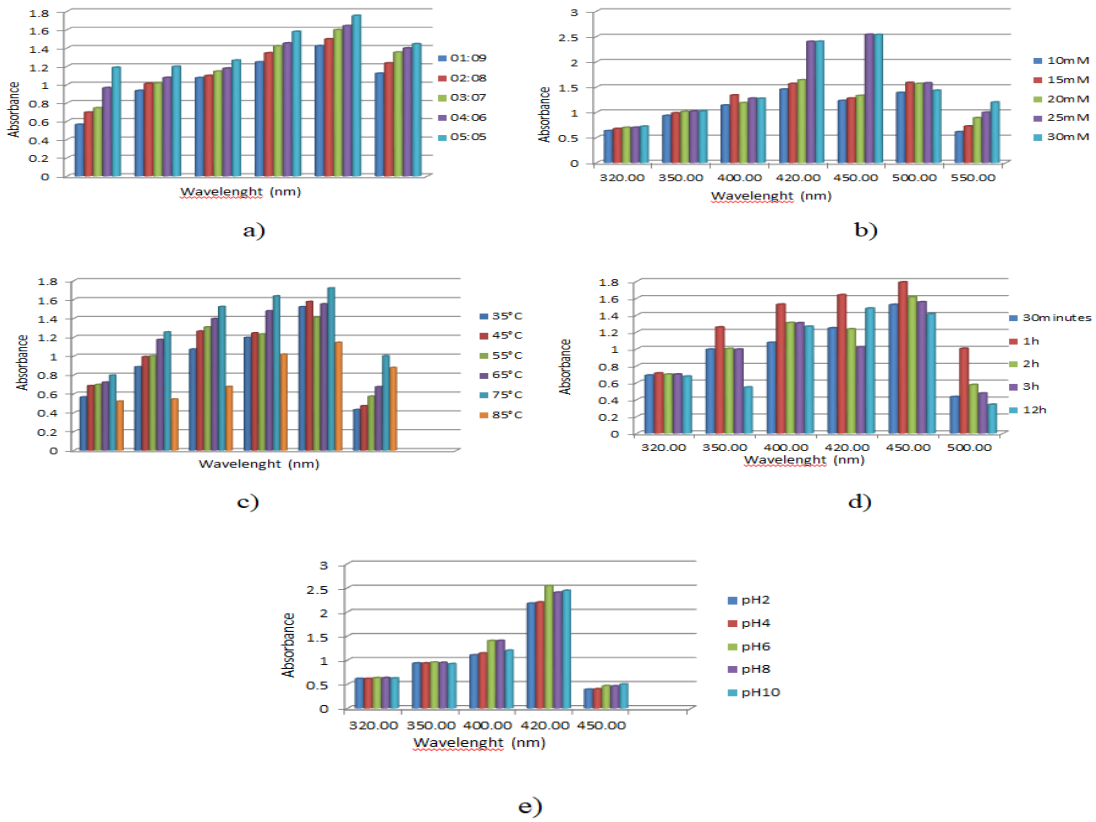

Figure 2: Optimization of different parameters a) Effect of ratio of leaf extract and copper zinc solution b) Effect of concentration of Cu-Zn nps c) Effect of temperature d) Effect of reaction time e) Effect of pH

Maximum absorption in the UV-Vis spectra was used to confirm maximum nanoparticle formation. With the increase in reaction time, UV-Vis spectra show sharp narrow peak after 3h which indicates the maximum formation of nanoparticles. This single, strong band shows that the particles have isotropic shape and uniform size. Stability of nanoparticles ensures that nanoparticles can be used for a long time[41].

Higher concentrations or ratios of reducing agent to substrate expedite the reduction process, which is then followed by a capping agent to avoid aggregation. Changes in absorption peak in that reaction mixture were observed with varying or choosing different salt concentration from 10mM to 25mM. The maximum peak intensity was obtained at 25mM of Cu-Zn salt. Size and shape of nanoparticles are subjected to change according to change in concentration of plant extract from 1ml to 5ml in 25mM Cu-Zn solution of volume in 100 ml. When we increase the volume of extract of plant leaves, the sample absorbance increased which in turn depicts that the on increasing the concentration of plant extract the Cu-Zn particle size gets reduced[27].

pH and temperature are physical characteristics that influence nanoparticle form. Temperature plays a critical role in synthesis of nanoparticles and also on size and shape of nanoparticles synthesized. The temperature was varied from 35°C to 75°C at an interval of 10°C. When temperature was increased, an increase in nanoparticle synthesis was observed in the reaction mixture, which again depends on faster reduction rate of Cu-Zn ions depicted by change in color from green to dark bluish green within minutes. Optimum temperature was obtained for our experiment as 75°C. Whereas on increasing temperature further above 75°C, the absorbance peak broadens which shows increased particle size[27].

pH changes affect particle shape and size because pH can alter the charge of biomolecules, affecting their capping and stabilizing abilities. The effects of pH on the biosynthesis of Cu-Zn NPs were investigated for the optimum conditions for producing Cu-Zn NPs. At low pH 2, no nanoparticles are formed. The intensity of absorption increases as the pH rises from 2 to 8, but it lowers again at pH 10. The results revealed that pH 8 had a significant impact on the size of the nanoparticle. It appears that at lower pH values, the rate of nucleation is considerably higher, resulting in a large number of Cu-Zn nuclei and as a result, delayed expansion of the Cu-Zn lattices[9].

UV-Vis spectrophotometer analysis: The electromagnetic induction excited the free conduction band electrons whose surface resonance results in absorptions of NPs on certain wavelength under UV- spectroscopy. This resonance was observed because the incident light wavelength exceeded the particle diameter. Optical properties of monometallic and bimetallic nanoparticle were studied using UV-Vis spectrophotometer analysis. UV spectra of monometallic and bimetallic nanoparticle are given in figure 3. Zn NPs resulted in absorption peaks in the UV-Vis spectrum at 398nm[28]. Surface Plasmon absorption of the metal oxide resulted in these peaks[21]. The reduction of Cu nanoparticles was confirmed by using UV-Vis spectrum which showed a distinct peak at 570nm[17].

The UV-visible spectrum of Cu–Zn nanoparticles exhibited a distinct peak 437nm. There were no further peaks in the UV-Vis spectra, indicating that nanoparticle agglomeration was either absent or minimal. These findings are consistent with previous research by Elumalai and Velmurugan who studied the green manufacturing of monometallic zinc Nps using *Lantana camara* leaf extract similar to present report except that bimetallic NPs were synthesized in investigation. Furthermore, the outcomes of this green synthesis approach for Zn-NPs are consistent with the observations made by Parthasarathy et al[30]. Similar to present study, Tiwari et al[43] studied the UV–Vis spectrum of the green synthesized ZnO NPs revealing two prominent absorption peaks at 355 nm and 370 nm with energy band gap of 2.986 eV.

XRD analysis: XRD is used for characterization of nanoparticles of any sizes and the observed changes in positions of diffraction peaks are used to make conclusions on how crystal structure and cell parameters change with the change in nanoparticles shape and size. Diffraction peaks for copper nanoparticles (Figure 4, Graph b) were observed at 28.55, 32.02, 38.72, 42.99 and 44.38 of 2θ which correspond to (101), (103), (004), (112) and (200) crystal planes and in good coordination with JCPDS[8,12]. Diffraction peaks for zinc nanoparticles (Figure 4 Graph-a) were observed at 26.91, 31.80, 34.37, 36.24, 39.81 and 48.41 of 2θ which correspond to (002), (101), (103), (004), (112) and (200) crystal planes[2].

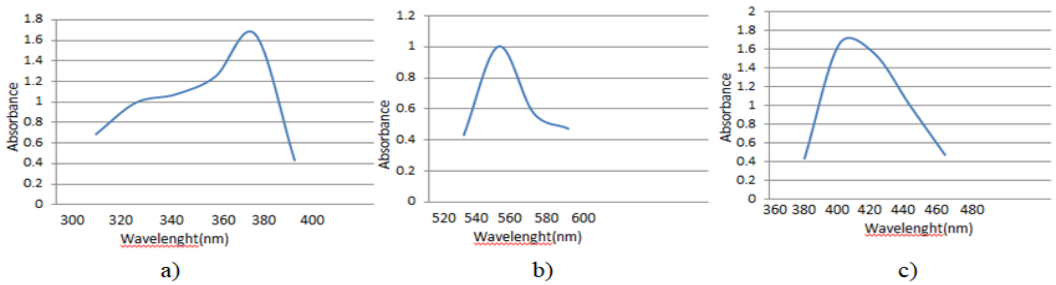

Figure 3: UV- visible spectrum observed for Zn, Cu and Cu-Zn nanoparticles

Table 1
Comparative analysis of XRD spectrum of a) Zn b) Cu and c)Cu-Zn nanoparticles

Sr.no	2 thetha	FWHM	d-space	C.Size	Average(nm)
1.	26.91851	0.35732	3.3095	22.860838	18.760
2.	31.80849	0.48112	2.7275	17.212752	
3.	34.3744	0.404	2.6068	20.583238	
4.	36.24609	0.30656	2.3513	27.427848	
5.	39.81505	0.38071	2.2622	22.193226	
6.	48.41541	3.80308	1.8785	2.2903074	

a)

Sr.no	2 thetha	FWHM	d-space	C.Size	Average(nm)
1.	28.55791	0.68196	0.18998	12.020559	37.086
2.	32.0212	6.10688	0.21246	1.3533716	
3.	38.71135	11.0050	0.26794	0.7699624	
4.	42.99977	0.92937	0.20585	8.8706537	
5.	44.38212	9.09138	0.29093	0.9437289	

b)

Sr no.	2theta	FWHM	d-space	C.size	Average
1.	22.80438	0.84049	2.11551	14.80876	14.45043759
2.	31.2907	0.72421	2.767206	20.92970	
3.	36.7069	0.576	2.541202	11.51118	
4.	38.8591	0.45231	1.899101	19.21548	
5.	48.42886	1.51119	1.8424	5.787052	

c)

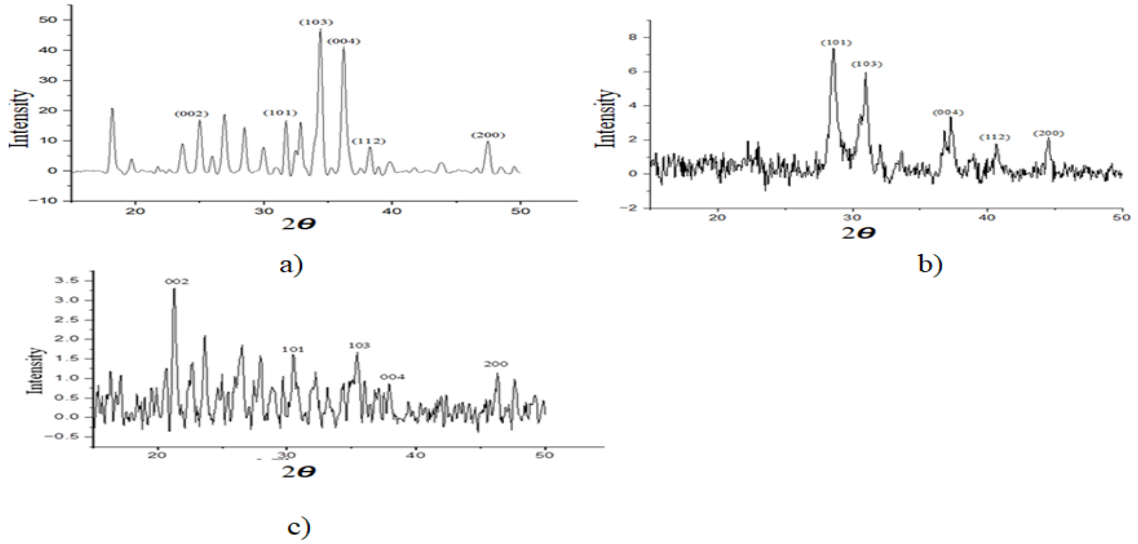

Figure 4: Comparative analysis of XRD spectrum of a)Zn nps b) Cu nps c)Cu-Zn nanoparticles

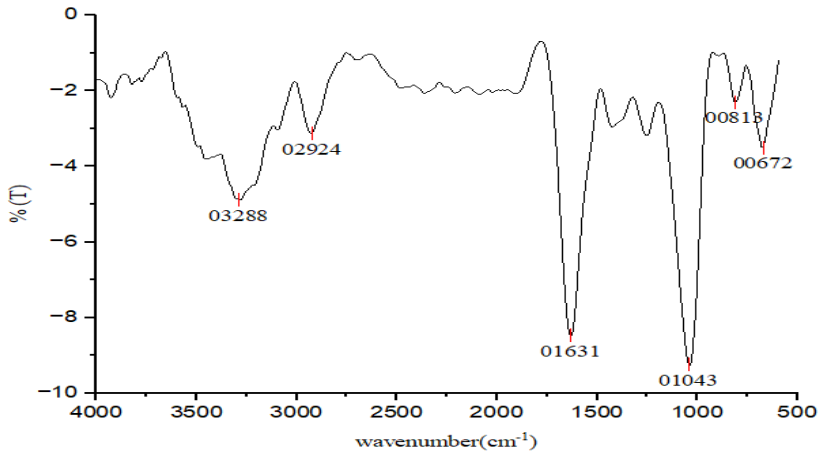

Figure 5: FTIR analysis of Cu-Zn nanoparticles synthesized

Diffraction peaks for Copper-Zinc nanoparticles (Graph-c) were observed at 22.80, 31.29(Zn), 36.70(Zn), 38.85(Cu) and 48.42 (Zn) of 2θ which correspond to (002), (101), (103), (004) and (200) crystal planes for copper and zinc nanoparticles respectively which were in good agreement with reference to the unit cell of face-centered-cubic structure by comparing with JCPDS (Joint Committee for powder diffraction standards) data.

Apart from these peaks responsible for nanoparticles, the recorded XRD pattern shows additional unassigned peaks owing to formation of the crystalline bioorganic compounds/metalloproteins that are present in the plant extract**.** Tiwari et al[43] and Daimari et al[5] reported similar XRD analysis results with particle sizes ranging from 7 to 23 nm with an average size of 16.49 nm.

Fourier Transform Infrared (FTIR): FTIR analysis scanned the samples for inorganic, organic and polymeric material used for the identification utilizing infrared light. FTIR analysis was utilized to identify the functional groups on the surface of the produced nanoparticles. The FTIR was carried out between the wavelength 500 cm^{-1} to 4000 cm^{-1}. The strong peaks were observed at 3288cm^{-1}, 2924cm^{-1}, 2129cm^{-1}, 1599cm^{-1}, 1427cm^{-1}, 1043$cm^{-1}$and 672cm^{-1} in FTIR spectrum of copper zinc nanoparticles synthesized by leaf extract as shown in figure 5. Broad peak obtained at 3288 corresponded to OH stretching vibrations, peak in the range of 1599 and 1427 corresponded to C=C stretch in aromatic ring and C=O stretch in polyphenols and C–N stretch of amide-I in protein.

Weak peaks obtained at 1043 and 672 demonstrated the presence of C–O stretching in amino acid, C–N stretching and C–H bending respectively similar to study of Iashin et al[16]. The spectra of fungal medium filtrate bands at 3263, 2940, 2861, 1719, 1577, 1386 and 1031 cm^{-1} referred to hydroxyl groups vibration stretching, C–H groups asymmetric stretching vibration of aliphatic groups and polyphenol skeleton of aromatic structures[15].

Field emission Scanning electron microscope (FESEM): FESEM analysis is done to visualize shape and size of nanoparticle. FESEM images showed that nanoparticles were irregular and range from 10-80 nm with average size of 38.28nm, σ=15.79 in figure 6 when analysed using Image J software. Singh et al[39] reported the SEM image in a bimetallic with metallic shiny particle aggregated with a size lower than 50 nm.

Energy Dispersive Spectroscopy (EDS): EDS was used to elucidate the elemental composition of copper-zinc nanoparticle, as illustrated in figure 7. The obtained EDS analysis showed the copper and zinc amount of 79.79 and 20.21 wt% respectively. The revelation of carbon in the plant extract confirmed the eco-friendly synthesis approach and highlighted the impact of natural components on the final composition. Elemental mapping of BNPs as shown in figure 8 revealed that Zn and Cu NPs were consistently dispersed and confined within a well-defined area, suggesting a well-controlled synthesis process with precise nanoparticle arrangement.

Carbon identified during mapping could be derived from the plant extract utilized in the manufacturing process. The mapping reveals a reciprocal interaction between Zn and Cu NPs, which explains their diverse geographical distribution. These patterns revealed a close link and shed light on the cooperative action that happened during BNP formation. Cao et al[3] and Daimari et al[5] reported comparable results, with weight percentages of Zn, Cu and O-atoms detected in bimetallic nanoparticles green synthesised from *Eryngium foetidum* leaf extract of 34.28%, 30.12% and 25.06%.

Zeta potential particle size analysis: The particle size and Zeta potential of green synthesized Cu, Zn and Cu-Zn were determined in an aqueous solution using a particle size analyser. The PDI parameter is used to assess the homogeneity of nanoparticles. The size distribution and Zeta potential of the prepared Cu, Zn and Cu-Zn nanoparticles were measured at temperature 24.54°C, 25.85°C and 25.04°C. The polydispersity index (PdI) of synthesized Cu, Zn and Cu-Zn nanoparticles was below 0.486, 0.344 and 0.243 with net surface charge of -35.56, -34.87 and 34.13mV which infers to the stability of nanoparticles in figure 9. It is well known that the size and charge on surface distribution play key roles in the biological activity of prepared NPs[23,24].

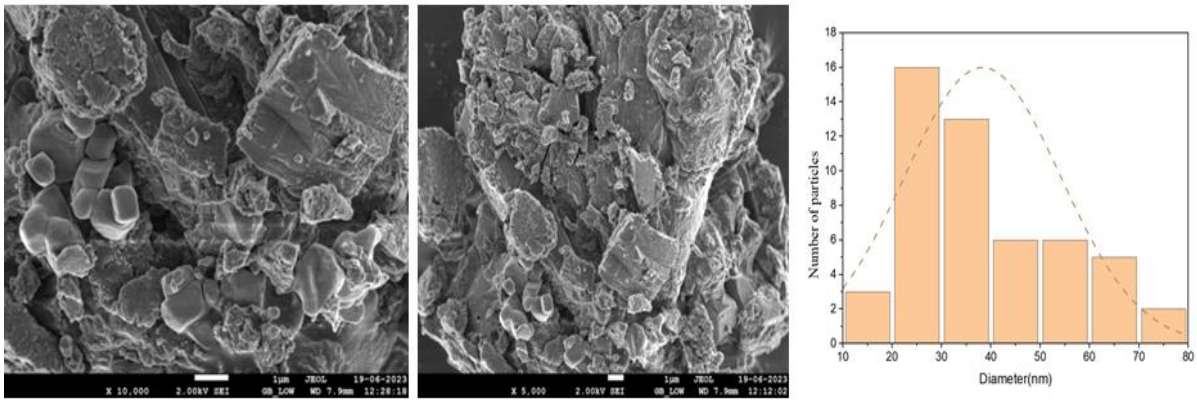

Figure 6: Field emission Scanning electron microscope analysis of Cu-Zn nanoparticles

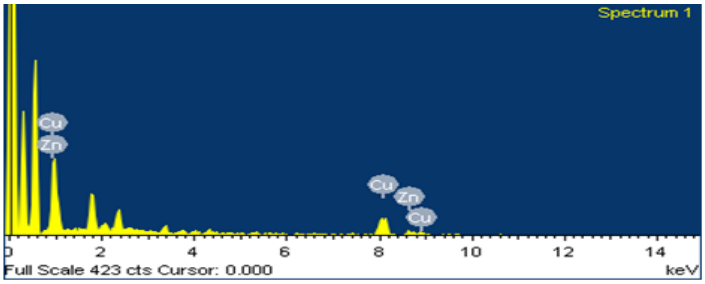

Element	Weight%	Atomic%
Cu K	79.79	80.25
Zn K	20.21	19.75
Totals	100.00	

Figure 7: EDS spectrum of synthesised copper-zinc nanoparticles

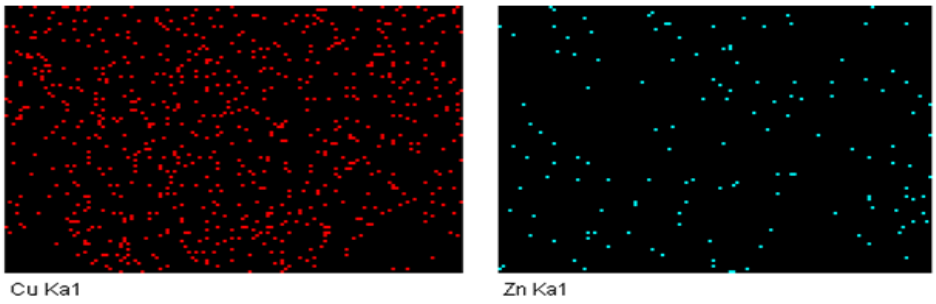

Figure 8: EDS elemental Mapping of copper-zinc nanoparticles

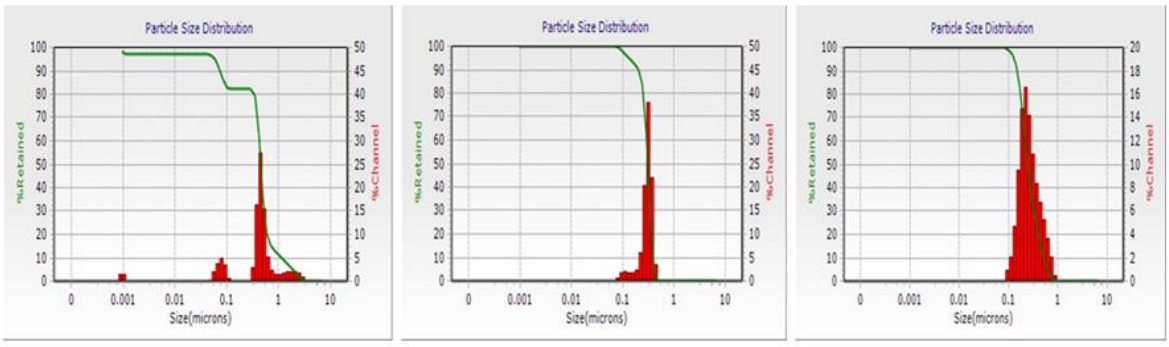

Figure 9: Zeta potential of a) Zn nanoparticles b) Cu nanoparticle c) Cu-Zn nanoparticle

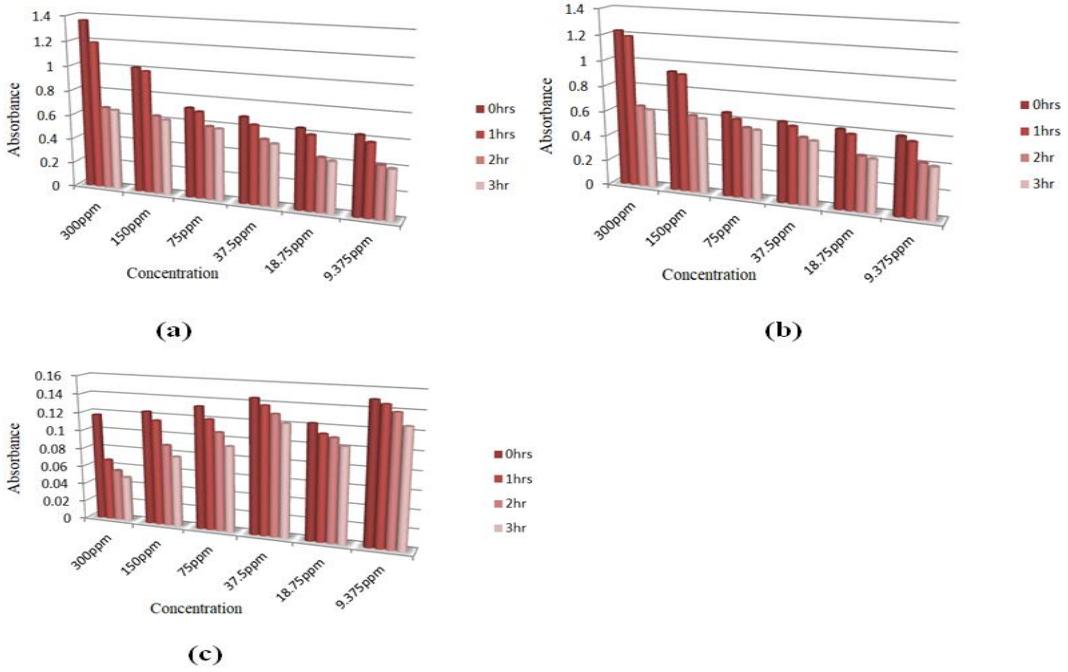

Figure 10: Dye degradation activity of a) Cu nanoparticle b) Zn nanoparticle c) Cu-Zn nanoparticle

Dye Degradation Activity: One of the efficient applications of Cu, Zn and Cu-Zn NPs is dye degradation. Congo red is an extremely toxic and non-biodegradable azo dye. It is primarily derived from dyeing companies that pollute water. This has a deleterious impact on the aquatic ecosystem's balance. In the present investigation, different concentrations of the synthesized Cu, Zn and Cu-Zn NPs had been applied over the dye for its degradation. The results are shown in figure 10.

From the UV-Vis plot within 2 hours, degradation of dye using nanoparticles was observed. The absorption peak of the dye molecules gradually decreases as the time passes, when the absorption peak disappears, the color of the solution changes from red to colourless. Complete dye degradation was not detected; only a maximum of 50% degradation was noted. The Congo red degradation reaction was monitored by UV-Vis spectrophotometer at 498 nm. Kolya et al[19] and Ahsani-Namin et al[1] demonstrated azo dye (Congo red) degradation utilising *Amaranthus gangeticus*-derived silver nanoparticles and the synthesis of copper zinc oxide using *Eryngium planum* plant extract as a natural green fuel demonstrating remarkable adsorption capacity for Congo red dye. Rani et al[37] reported the elimination of organic dyes with green synthesis silver nanoparticles.

Conclusion

Zinc, copper and bimetallic copper zinc nanoparticles were successfully synthesized using *Lantana camara* leaf extract and subjected to a comprehensive characterization employing modern analytical techniques. Reduction of the monometallic and bimetallic during exposure, followed color change of the solution from blue to light bluish green, colourless to light yellow, bluish solution to dark green colored solution of Cu, Zn and copper-zinc. Optimization of some parameters was also done for the efficient formation of Cu-Zn nanoparticles. X-ray diffraction (XRD) analysis unequivocally confirmed the crystalline nature of the Zn, Cu and Cu-Zn -NPs, revealing an average particle size of 18.7, 37.0 and 14.4 nm.

Further insights from Field emission scanning electron microscopy (FESEM) elucidated that the nanoparticles exhibited an irregular shaped with agglomeration, displaying particle sizes ranging around 38.8 nm. The polydispersity index (PdI) of synthesized Cu, Zn and Cu-Zn nanoparticles was below 0.486, 0.344 and 0.243 with net surface charge of -35.56, -34.87 and 34.13mV which infers to the stability of nanoparticles. UV-Vis spectroscopy provided corroborating evidence, affirming the optical properties of the Zn, Cu and Cu-Zn -NPs with an observed absorption peak at 398, 570 and 437 nm.

Because of this reason, synthesizing metallic nanoparticles, especially by non-toxic green synthesis method, is used in many application fields such as cancer treatment, drug transport, biosensor construction which are of great importance today. These compelling findings hold significant promise for potential agricultural applications aimed at enhancing seed germination rates and superior capacity for enhancing seedling growth and overall yield. By utilizing these findings, agricultural practices could be further advanced to contribute to improved crop production and sustainable agricultural practices.

References

1. Ahsani-Namin Z., Norouzbeigi R. and Shayesteh H., Green mediated combustion synthesis of copper zinc oxide using *Eryngium planum* leaf extract as a natural green fuel: Excellent adsorption capacity towards Congo red dye, *Ceram. Int.*, **48(14)**, 20961-20973 **(2022)**

2. Ayoub I.M., El-Shazly M., Lu M.C. and Singab A.N.B., Antimicrobial and cytotoxic activities of the crude extracts of Dietes bicolor leaves, flowers and rhizomes, *S. Afr. J. Bot.*, **95**, 97-101 **(2014)**

3. Cao Y. et al, Green synthesis of bimetallic ZnO–CuO nanoparticles and their cytotoxicity properties, *Sci. Rep.*, **11**, 23479 **(2021)**

4. Chung I.M., Rahuman A.A., Marimuthu S., Kirthi A.V., Anbarasan K. and Padmini P., Green synthesis of copper nanoparticles using *Eclipta prostrata* leaves extract and their antioxidant and cytotoxic activities, *Exp Ther Med*, **14**, 18–24 **(2017)**

5. Daimari J. and Deka A.K., Anticancer, antimicrobial and antioxidant activity of CuO–ZnO bimetallic nanoparticles: green synthesised from *Eryngium foetidum* leaf extract, *Sci. Rep.*, **14(1)**, 19506 **(2024)**

6. Danbature W.L., Shehu Z., Yoro M. and Adam M.M., Nanolarvicidal effect of green synthesized Ag-Co bimetallic nanoparticles on *Culex quinquefasciatus* mosquito, *Adv. Biol. Chem*, **10(1)**, 16-45 **(2020)**

7. Daphedar A. and Taranath T.C., Green synthesis of zinc nanoparticles using leaf extract of Albizia saman (Jacq.) Merr and their effect on root meristems of Drimia indica (Roxb.) Jessop, *Caryologia*, **71**, 91–102 **(2018)**

8. Davydova L., Menshova A., Shumatbaev G., Babaev V. and Nikitin E., Phytochemical Study of Ethanol Extract of *Gnaphalium uliginosum* L. and Evaluation of Its Antimicrobial Activity, *Antibiotics*, **13(8)**, 785 **(2024)**

9. Dejene A., Bogale R.F., Yadeta L., Gendo K.M., Kenasa G. and Berhanu A.L., Biogenic synthesis of copper oxide nanoparticles using Clausena anisata leaf and Euphorbia abyssinica bark extracts and its comparative study of antibacterial activities, *Results Chem.*, **8**, 101569 **(2024)**

10. Dulta K., Ağçeli G.K., Chauhan P. and Chauhan P.K., Biogenic production and characterization of CuO nanoparticles by Carica papaya leaves and its biocompatibility applications, *J. Inorg. Organomet. Polym. Mater*, **31(4)**, 1846-1857 **(2021)**

11. Elumalai K. and Velmurugan S., Green synthesis, characterization and antimicrobial activities of zinc oxide nanoparticles from the leaf extract of *Azadirachta indica* (L.), *Applied Surface Science*, **1(345)**, 329-36 **(2015)**

12. Fang J. and Xuan Y., Investigation of optical absorption and photothermal conversion characteristics of binary CuO/ZnO nanofuids, *RSC Adv.*, **7**, 56023–56033 **(2017)**

13. Ghisalberti E.L., Lantana camara L. (verbenaceae), *Fitoterapia*, **71(5)**, 467-486 **(2000)**

14. Harborne J.B., The biochemical systematics of flavonoids, In the flavonoids, Springer US, 1056–1095 **(1975)**

15. Hasanin M.S., Hashem A.H., Al-Askar A.A., Haponiuk J. and Saied E., A novel nanocomposite based on mycosynthesized bimetallic zinc-copperoxide nanoparticles, nanocellulose and chitosan: characterization, antimicrobial and photocatalytic activities, *Electron. J. Biotechnol*, **65**, 45-55 **(2023)**

16. Iashin I. et al, Green biosynthesis of zinc and selenium oxide nanoparticles using callus extract of Ziziphus spina-christi: Characterization, antimicrobial and antioxidant activity, *Biomass Convers Biorefin*, https://doi.org/10.1007/s13399-021-01873-4 **(2021)**

17. Kasthuri K., Kumar J.K., Rajkumar P., Kalpana S. and Balasubramani V., Feasible antibacterial nanomaterials: Copper oxide nanoparticles synthesized using dandelion leaf extract, *Inorg. Chem. Commun.*, **167**, 112804 **(2024)**

18. Khatak S., Wadhwa N. and Jai, Monometallic zinc and bimetallic Cu-Zn nanoparticles synthesis using stem extracts of *Cissus quadrangularis* (Haddjod) and Proneness as alternative antimicrobial agents, *Biosci Biotechnol Res Asia*, **17(4)**, 763-774 **(2020)**

19. Kolya H., Maiti P., Pandey A. and Tripathy T., Green synthesis of silver nanoparticles with antimicrobial and azo dye (Congo red) degradation properties using *Amaranthus gangeticus* Linn leaf extract, *Journal of Analytical Science and Technology*, **6**, 1-7 **(2015)**

20. Kumar S., Sandhir R. and Ojha S., Evaluation of antioxidant activity and total phenol in different varieties of *Lantana camara* leaves, *BMC Research Notes*, **7**, 1-9 **(2014)**

21. Kyene M.O., Droepenu E.K., Ayertey F., Yeboah G.N., Archer M.A., Kumadoh D. and Appiah A.A., Synthesis and characterization of ZnO nanomaterial from Cassia sieberiana and determination of its anti-inflammatory, antioxidant and antimicrobial activities, *Scientific African*, **19**, e01452 **(2023)**

22. Lobo D.A., Velayudhan R., Chatterjee P., Kohli H. and Hotez P.J., The neglected tropical diseases of India and South Asia: review of their prevalence, distribution and control or elimination, *PLoS Neglected Tropical Diseases*, **5(10)**, e1222 **(2011)**

23. Lozhkomoev A.S., Bakina O.V., Pervikov A.V., Kazantsev S.O. and Glazkova E.A., Synthesis of CuO–ZnO composite nanoparticles by electrical explosion of wires and their antibacterial activities, *J Mater. Sci: Mater. Electron*, **30**, 13209-13216 **(2019)**

24. Mendez-Trujillo V., Valdez-Salas B., Carrillo-Beltran M., Curiel-Alvarez M.A., Tzintzun-Camacho O., Ceceña-Duran C. and Gonzalez-Mendoza D., Green synthesis of bimetallic nanoparticles from *Prosopis juliflora* (Sw) DC. and its effect against cotton mealybug, Phenacoccus solenopsis (Hemiptera: Pseudococcidae), *Phyton*, **88(3)**, 269 **(2019)**

25. Moellering Jr. R.C., Graybill J.R., McGowan Jr. J.E. and Corey L., Antimicrobial resistance prevention initiative—an update: proceedings of an expert panel on resistance, *Am. J. of Infect. Control*, **35(9)**, S1-S23 **(2007)**

26. Mohanty S.K., Mallappa K.S., Godavarthi A., Subbanarasiman B. and Maniyam A., Evaluation of antioxidant, in vitro cytotoxicity of micropropagated and naturally grown plants of Leptadenia reticulata (Retz.) Wight & Arn.-an endangered medicinal plant, *Asian Pac J. Trop. Med.*, **7**, S267-S271 **(2014)**

27. Muniz F.T.L., Miranda M.R., Morilla dos Santos C. and Sasaki J.M., The Scherrer equation and the dynamical theory of X-ray diffraction, *Acta Crystallographica Sec A Foundation Adv*., **72(3)**, 385–90, https://doi.org/10.1 25 **(2016)**

28. Mydeen S.S., Kumar R.R., Kottaisamy M. and Vasantha V.S., Biosynthesis of ZnO nanoparticles through extract from Prosopis julifora plant leaf: Antibacterial activities and a new approach by rust-induced photocatalysis, *J Saudi Chem Soc.*, **24(5)**, 393–406, https://doi.org/10.1016/j.jscs. 2020.03.003 **(2020)**

29. Nahar K., Aziz S., Bashar M., Haque M.A. and Al-Reza S.M., Synthesis and characterization of Silver nanoparticles from *Cinnamomum tamala* leaf extract and its antibacterial potential, *Int. J. Nano Dimens*, **11(1)**, 88-98 **(2020)**

30. Natrayan L., Janardhan G., Nadh V.S., Srinivas C., Kaliappan S. and Velmurugan G., Eco-friendly zinc oxide nanoparticles from *Moringa oleifera* leaf extract for photocatalytic and antibacterial applications, *Clean Technol. Environ. Policy*, **27**, 1–13 **(2024)**

31. Palei N.N., Green synthesis of silver nanoparticles using leaf extract of *Lantana camara* and its antimicrobial activity, *Int. J. Green Pharm.*, **14(2)**, 1-7 **(2020)**

32. Parrotta J.A., Healing Plants of Peninsular India, CAB International, Wallingford, UK and New York, 944 **(2001)**

33. Parthasarathy G., Chen J., Chen X., Chia N., O'Connor H.M., Wolf P.G., Gaskins H.R. and Bharucha A.E., Relationship between microbiota of the colonic mucosa vs feces and symptoms, colonic transit and methane production in female patients with chronic constipation, *Gastroenterology*, **150(2)**, 367-79 **(2016)**

34. Patel S., A weed with multiple utility: Lantana camara, *Reviews in Environ. Bio/Technol.*, **10**, 341-351 **(2011)**

35. Rajoriya P., Green synthesis of silver nanoparticles, their characterization and antimicrobial potential, Ph.D. Thesis, Sam Higgin bottom University of Agriculture, Technology & Sciences **(2017)**

36. Ramesh P., Rajendran A. and Meenakshisundaram M., Green syntheis of zinc oxide nanoparticles using flower extract *cassia auriculata*, *J. Nano Sci. Nano Technol.*, **2(1)**, 41-45 **(2014)**

37. Rani G., Bala A., Ahlawat R., Nunach A. and Chahar S., Recent Advances in Synthesis of AgNPs and Their Role in Degradation of Organic Dyes, Comments on *Inorg. Chem*, **45(1)**, 1-29 **(2024)**

38. Sariwahyuni, Fitri Junianti and Rianti Indah Lestari, Utilization of Coconut Pulp as Raw Material for Bioethanol Production, *Res. J. Chem. Environ.*, **27(12)**, 57-63 **(2023)**

39. Singh G. and Devi T., Studies on photocatalytic mineralization of organic pesticides by bimetallic Cu-Zn nanoparticles derived from Roscoe (ginger) using green chemistry approach, *Environ. Sci. Pollut. Res. Int*., **31(19)**, 27699-27708 **(2024)**

40. Singh P.P., Chaturvedi S., Bhatnagar T., Das S. and Debnath N., Green synthesis of ZnO nanoparticles using *Lantana camara* leaf extract for the enhancement of plant growth, *Adv. Nat. Sci. Nanosci. Nanotechnology*, **15(3)**, 035010 **(2024)**

41. Sukumar S., Rudrasenan A. and Padmanabhan Nambiar D., Green-synthesized rice-shaped copper oxide nanoparticles using *Caesalpinia bonducella* seed extract and their applications, *ACS Omega*, **5(2)**, 1040-1051 **(2020)**

42. Swamy M.K. and Sinniah U.R., A comprehensive review on the phytochemical constituents and pharmacological activities of Pogostemon cablin Benth.: an aromatic medicinal plant of industrial importance, *Molecules*, **20(5)**, 8521-8547 **(2015)**

43. Tiwari A.K., Jha S., Tripathi S.K., Shukla R., Awasthi R.R., Bhardwaj A.K. and Dikshit A., Spectroscopic investigations of green synthesized zinc oxide nanoparticles (ZnO NPs): antioxidant and antibacterial activity, *Discover Applied Sciences*, **6(8)**, 399 **(2024)**

44. Venkatachalam T., Kumar V.K., Selvi P.K., Maske A.O. and Kumar N.S., Physicochemical and preliminary phytochemical studies on the *Lantana camara* (L.) fruits, *Int. J. Pharm. Pharm. Sci.*, **3(1)**, 52-54 **(2011)**

45. Vijayaraghavan K., Nalini S.P.K., Prakash N.U. and Madhankumar D., Biomimetic synthesis of silver nanoparticles by aqueous extract of *Syzygium aromaticum*, *Mat. Lett*., **75**, 33-35 **(2012)**.

(Received 13th December 2024, accepted 14th February 2025)